The role of intraspecific competition during post-glacial recolonization: a Norway spruce case study

Tiret M., Zhou L., Scheepers G., Grahn T., Karlsson B., Milesi P., Lascoux M., Lundqvist SO., García-Gil MR

Abstract: During the climate warming after the last glaciation event, many plant species underwent an expansion that still today shapes their current distribution and population structure. Norway spruce was no exception, and its current distribution is the result of a complex demographic history. Recolonization abilities depend on the competitive ability, but little is known about the shaping force of competition during post-glacial expansions in tree species. In the present study, we investigated the different competitive abilities of the post-glacial genetic clusters of Norway spruce. We assessed the adaptations underlying the trunk diameter, wood density and tracheid traits using a large dataset of 4,461 individuals from 396 half-sib families, 118,145 SNPs from, mixed linear models and multiple Genome-Wide Association Studies, in the progeny tests implemented by the Swedish breeding program. We show that (i) in terms of competition, macroscopic traits are what matters, much more so than tracheid dimensions; (ii) the ability to benefit from early competition is stronger in core populations or ancient refugia; and (iii) population structure for Norway spruce is intrinsically associated with latitude, and as such is a good predictor of adaptation but an impediment for detecting underlying genetic variants.

keywords: norway spruce, wood properties, adaptation, population structure, early competition, GWAS.

Introduction

During the last Quaternary glaciation event, the distributions of many animal and plant species were shifted towards restricted small refugia (Bennet, 1997). Comparative analyses of genetic variations revealed that, during the glaciation period, most of the species in Europe were confined into the Iberian, Italian and Balkan peninsulas (Hewitt, 2008; Provan & Bennet, 2008). Resulting in strong founder effects, these severe bottlenecks still shape today the distribution and the population structure of current species (Hewitt, 1996; Hewitt, 2000). During the post-glacial period, extant species underwent an expansion that resulted in a mixture of admixture from different refugia (e.g., Petit et al., 2003), natural selection to new environments (e.g., Saccheri & Hanski, 2006), and inter or intraspecific competition (e.g., Case et al., 2005). The match between post-glacial migration routes and current distributions was unraveled for many tree species (e.g., Vendramin et al., 2000; Petit et al., 2002; Palmé & Su et al., 2003), and the current distribution of Norway spruce (Picea abies (L.) H. Karst.) was no exception. Norway spruce thrives nowadays in a vast northern domain ranging from Norway to central Russia, and in two smaller domains, Alpine and Carpathian (Tsuda et al., 2016). Recent demographic movements led the Norway spruce to be divided into seven genetic clusters (Chen et al., 2019): Central and South Sweden (CSE), Russia-Baltics (RBA), Northern Poland (NPL), Central Europe (CEU), Alpines (ALP), Carpathian (ROM), and hybrids between CSE and ALP (CSE-ALP).

During a (re)colonization or expansion, a trade-off is expected between the dispersal and the competitive abilities (Burton et al., 2010). Apart from few studies (e.g., Case et al., 2004; Sedmakova et al., 2019), little is known about the shaping force of competition during post-glacial expansions in tree species. To get a comprehensive picture of post-glacial expansion of Norway spruce, we investigated the adaptations underlying the diameter at breast height (DBH) as a proxy of the global size of the tree, and wood density as an easy to measure and good summary of wood properties. DBH and wood density are both tightly linked to competition, as the former is a proxy of the upright growth, giving the competitive advantage in the acquisition of light resources, and the latter provides the necessary mechanical support to the former (Givnish, 1982; Iwasa et al., 1985; Falster 2003, Falster & Westoby, 2005; Chave et al., 2009). Both are also tightly linked in the so-called growth-survival trade-off, where low wood density is associated with fast growth rates, whereas high wood density is associated with high survival rates (Kitajima, 1994; Enquist, 1999; van Gelder et al., 2006; Poorter et al., 2010). Additionally, to account for different growth-survival trade-offs in different stages of life, we analyzed DBH and wood density on consecutive annual rings, where the pith-to-bark pattern unravels the early and later stages of the tree lifespan. We also incorporated in the analyses measures of tracheid dimensions to assess how deep the competition can affect tree phenotypes.

In order to confidently infer signals of adaptation, a notoriously efficient approach to rule out environment and plastic effects is through common gardens (Savolainen et al., 2013; de Villemereuil et al., 2020). Since the Swedish breeding program is a mixture of local trees and recent introductions from other European countries, the progeny tests, although incomplete, constitute a prominent resource of information in the form of common gardens (Chen et al., 2019; Milesi et al., 2019). Nowadays, breeding programs are the main sources of phenotypic

data, and as such, become increasingly valuable for genomic studies. Using then the Swedish breeding program, we assessed the competitive abilities of the different post-glacial clusters of Norway spruce with a large dataset of 4,461 individuals from 396 half-sib families, 118,145 SNPs from a target resequencing exome capture, mixed linear models and multiple Genome-Wide Association Studies. We show that (i) in terms of competition, macroscopic traits - DBH and wood density - are what matters, much more so than tracheid dimensions; (ii) the ability to benefit from early competition is stronger in core populations or ancient refugia; and (iii) population structure for Norway spruce is intrinsically associated with latitude, and as such is a good predictor of adaptation but an impediment for detecting underlying genetic variants.

Materials and Methods

Plant materials. The study was conducted on two Skogforsk progeny test trials of Norway spruce at two different sites: S21F9021146 alias FF1146 (Höreda, Sweden; 57°60'N 15°04'E), and S21F9021147 alias FF1147 (Erikstorp, Sweden; 56°80'N 13°90'E). The trials were both established in the spring of 1990, with 1,373 half-sib families in FF1146 and 1,375 in FF1147, from open-pollinated seeds harvested on selected trees from 112 stands in southern Sweden. In both trials, a randomized incomplete block design was implemented (20 blocks in FF1146, 23 in FF1147), with single-tree plots in a homogeneous spacing of 1.4 m x 1.4 m. Commercial thinning occurred in 2008 at the age of 18, and in 2010 at the age of 20. After filtering out (i) half-sib families absent in the established Skogforsk clonal archives, and (ii) stands with less than three half-sib families, the study included a total of 517 half-sib families with 5,618 progenies (2,973 from FF1146, and 2,645 from FF1147).

Population structure was previously assessed at a fine scale by Chen et al. (2019), using 399,801 unlinked non-coding SNPs, categorizing families into the following genetic clusters (ordered by decreasing latitude): Central and South Sweden (CSE), Russia-Baltics (RBA), Northern Poland (NPL), Central Europe (CEU), Alpines (ALP), Carpathian (ROM), and hybrids between CSE and ALP (CSE-ALP) (for tree original location, see Fig. 1 of Milesi et al., 2019). The families considered in this study also followed the same genetic clustering (Fig. 1B, 1C). Individuals from the ROM genetic cluster were removed, as our sample consisted of only three of these families (as opposed to other genetic clusters constituted of at least ten families; Table S1).

Phenotype measurements. Increment cores of 12-mm diameter were collected in 2011 and 2012, at breast height (1.3 m), from six trees per half-sib family per trial, at calendar age 21 or 22, from the northern side of the stem. The dataset then only included trees of young ages, known to be the most dynamic phase (Lundqvist et al., 2018). The increment cores were then analyzed by SilviScan (RISE, Stockholm, Sweden), assessing high-resolution pith-to-bark radial variations in wood properties (Evans & Ilic, 2001). Annual rings were identified using the method of Lundqwist et al. (2018). For each core and each annual ring, we recorded the ring width (in mm), the wood density (in kg/m^3), and tracheid traits, such as the average tracheid radial width (TRW, in µm), the average tracheid tangential width (TTW, in µm), and the average tracheid wall thickness (TWT, in µm). From the ring width, we deduced the diameter at breast height (DBH, in mm) for each cambial age. Due to the variable growth rate, the offspring did not have the same number of annual rings at breast height (BH) - or namely, did not have the same cambial age at BH; we then also recorded the calendar age of an offspring when it reached BH, hereafter CBH.

The first two innermost annual rings and the outermost ring were removed due to measurement damages. To account for the varying number of offspring per ring of a specific cambial age, we only kept the third till the 13th ring. To avoid the effect of commercial thinning, we removed all annual rings recorded as having grown after 2008, and all individuals without any records in 2008. We then had six phenotypes per ring, at most 11 rings per offspring, and a measure of CBH per offspring.

Exome capture and SNP filtering. The exome capture (target re-sequencing) of the mother of each half-sib family is available on BioProject PRJNA511374 (Chen et al., 2019) and BioProject PRJNA731384 (Chen et al., 2021). Total genomic data were extracted from the buds of the 517 maternal trees (or needles when not available) using the Qiagen Plant DNA extraction kit (Qiagen, Germany). DNA concentration was assessed using the Qubit® ds DNA Broad Range Assay Kit (Oregon, USA). The extracted DNA was submitted to RAPiD Genomics (Gainesville, USA) for library preparation and exome sequencing. Sequence capture, with an average depth of 15X, was performed using the Illumina HiSeq 2500 (San Diego, USA), with 40,018 diploid probes (120bp-length) designed to capture 26,219 genes of P. abies (Vidalis et al., 2018). After mapping the raw reads against the P. abies reference genome v1.0 (Nystedt et al., 2013) using BWA-MEM with default settings (Li & Durbin, 2010), PCR duplicates were sorted and marked using SAMTOOLS v1.2 (Li et al., 2009) and Picard v1.141 (http://broadinstitute.github.io/picard). INDELs were realigned using GATK v3.5.0 (McKenna et al., 2010). Variant calling was performed using GATK HaplotypeCaller v3.6 (Van der Auwera et al., 2013), quality filtering was carried out by the Variant Quality Score Recalibration following the procedure of Van der Auwera et al. (2013), and non-biallelic SNPs were filtered out using GATK SelectVariants v3.6 (option --restrict-alleles-to BIALLELIC; Van der Auwera et al., 2010).

As an alternative way to account for Minor Allele Frequency (MAF), we filtered out SNPs with less than five families per genotype to avoid a leverage effect biasing the GWASs. We performed a loose filtering for variant call rate (or missingness) with PLINK v1.9 (Chang et al., 2015), by removing individuals with more than 70% missingness, resulting in 462 half-sib families, and by removing SNPs with more than 70% missingness, resulting in 118,145 SNPs (each mother is then covered by at least 35,443 SNPs). 70,277 SNPs were successfully mapped on the consensus map (Bernhardsson et al., 2019).

Statistical model. The following mixed model was considered to study the family effect underlying the phenotype at each annual ring:

$$Y_{ijkl} = \mu + s_i + B_{ij} + F_k + \varepsilon_{ijkl}, \qquad (1)$$

where 'Y_{ijkl}' is the phenotype of the l-th offspring of the k-th family in the j-th block at the i-th site, μ is the grand mean, 's_i' is the fixed effect of the i-th site, 'B_{ij}' and 'F_k' are uncorrelated random effects of the j-th block nested in i-th site (with variance σ_F^2) and the k-th half-sib family (with variance σ_B^2) respectively, and 'ε_{ijkl}' the residual fitted to a Gaussian distribution of variance σ^2. The family effect was not fitted using a kinship matrix, thus overestimating its effect and providing its upper bound. Heritability was estimated as $\sigma_F^2 / (\sigma_F^2 + \sigma_B^2 + \sigma^2)$. The estimated family effects were used as input for subsequent GWASs.

In addition, the following mixed model was considered to assess the effect of population structure on CBH:

$$Y_{ijkl} = \mu + s_i + g_k + B_{ij} + F_k + \varepsilon_{ijkl}, \qquad (1bis)$$

where 'g_k' is the fixed effect of the k-th family's genetic cluster, and the other terms are as defined above in the model (1). In order to further investigate the effect of CBH and genetic clusters on phenotypes, the following mixed model was considered:

$$Y_{ijkl} = \mu + c_l + s_i + g_k + (c \times g)_l + (c \times s)_l + B_{ij} + F_k + \varepsilon_{ijkl}, \qquad (2)$$

where 'c_l' is the fixed effect of the l-th offspring's CBH, '$(c \times g)_l$' is the fixed interaction effect between CBH and the genetic cluster of the l-th offspring, '$(c \times s)_l$' is the fixed interaction effect between CBH and the site of the l-th offspring, and the other terms are as defined above in the model (1bis). Each phenotype (DBH, wood density, ring width, TRW, TTW, and TWT) was normalized by its overall mean (Table 1) to allow comparison between phenotypes. The model (2) was applied on 66 phenotypes, as there were six phenotypes on 11 rings.

All computation was done using R - version 4.0.4 (R core team, 2021), and the models were fitted with the R package lme4 (function *lmer*; Bates et al., 2015). Statistical significance of the fixed effects was assessed using a type II Wald chi-square test (function *Anova* of the R package *car*), and significance of a slope was assessed using a Student *t*-test. Finally, to account for the unbalance caused by consecutive filtering, we only kept families with at least four offspring per site, resulting in at most 396 half-sib families and 4,461 offspring per phenotype.

Genome-Wide Association Study. GWAS was performed on the estimated family effect of model (1). We then fitted each SNP individually, with or without genetic clusters as a covariate. We also used the software GCTA (option --mlma; Yang et al., 2011) that included a polygenic effect (Supplementary material). GWAS not including kinship was referred to (M) when not corrected for population structure, and (M*) when corrected for population structure. GWAS including kinship (from GCTA) was referred to (K) when not corrected for population structure, and (K*) when corrected for population structure. GWAS (K*) would be the classic GWAS. For significant SNPs, we re-estimated the effect size by using an empirical Bayes approach for adaptive shrinkage with the R package *ashr* (function *ash*; Stephens, 2017).

In order to detect regions with high density of significant SNPs - namely peaks - we used a custom peak detection script with default settings (Tiret & Milesi, 2021), which is freely available at https://github.com/milesilab/peakdetection. On the other hand, in order to assess the quality of a GWAS through its Q-Q plot, we introduce the distance *D* as the distance between the highest log p-value (the rightmost value on a Q-Q plot) and the highest upper bound of the 95% confidence interval of a uniform distribution. If the distance D is positive, some SNPs are more significant than expected; if D is between 0 and −2.16 (the width of the confidence interval for n = 118,145), the p-value distribution follows a uniform distribution with a confidence level of 95%; and if D is below −2.16, the SNPs are less significant than expected, suggesting an overcorrection by population structure.

Results

The phenotypes were dominantly determined by the annual rings, the successive rings having similar profiles (Fig. 1A, S1-S3). The phenotypes that differed most between the rings were DBH and TTW (Peasrson $\rho = 0.63$; Fig.S2). Correlations between phenotypes remained constant over time, except for a slight decrease between DBH and TRW (from $\rho = 0.64$ to $\rho = 0.48$), and between DBH and wood density (from $\rho = -0.46$ to $\rho = -0.56$). As previously reported, southern populations had higher DBH and lower wood density (Rossi et al., 2014; Milesi et al., 2019). In addition, our dataset showed that southern populations had lower CBH and TWT, and higher ring widths, TRW and TTW (Table 1). The heritabilities of the 13th ring phenotypes ranged from 5.22% to 12.45% (Table 1), which are lower compared to previous reports (Hannrup et al., 2004; Chen et al., 2021). This is most likely due to the young age at which heritability was computed, as heritabilities increased over rings for all phenotypes. In addition, the common garden experiment showed evidence of competition, as DBH within blocks converged (Fig. S4), which is a typical response to competition.

CBH mostly impacts DBH in later rings and is population specific

CBH is determined by genetics and environment, as it was strongly explained by the site effect ($\chi^2 = 26.6$, degree of freedom = 5, $p = 3.05 \times 10^{-5}$) and the genetic cluster effect ($\chi^2 = 102.8$, df = 1, $p < 10^{-5}$) in the model (1bis). The environmental factor was slightly more pronounced, as suggested by a relatively lower heritability of 5.22% (Table 1). The genetic variance of CBH was however not low - in fact quite the opposite. Rather, CBH had a relatively higher environmental variance (Table 1). CBH also revealed a latitudinal component, where southern half-sib families had low CBH, i.e., fast growth rates (Fig. 2A). Despite the fact that CBH significantly depends on genetics and environment, other phenotypes were mostly related to CBH and its interaction with the site effect than to its interaction with the genetic cluster effect: in the model (2), at a Bonferroni adjusted cut-off of $p = 7.58 \times 10^{-3}$ (66 phenotypes), CBH and its interaction with the site effect were significant for 47 and 30 phenotypes respectively, while its interaction with the genetic cluster effect was significant for only 2 phenotypes (Table S2). For subsequent analyses, we focused only on the Höreda trial (the conclusions were the same in the Erikstorp trial).

Excluding ring width, the results showed that CBH mostly impacts early or later ring phenotypes (Fig.2B): in the model (2), at the same Bonferroni adjusted cut-off, CBH was significant for every phenotype at the 3rd and 4th rings but the 4th ring wood density ($\chi^2 = 7.77$, df = 1, $p = 5.32 \times 10^{-3}$), only for 6 out of 20 phenotypes between the 5th and the 8th rings ($\chi^2 > 16.4$, df = 1, $p < 1 \times 10^{-5}$), and for every phenotype at the 9th ring and beyond but the 9th ring TTW ($\chi^2 = 4.05$, df = 1, $p = 4.41 \times 10^{-2}$), the 11th ring TWT ($\chi^2 = 7.09$, df = 1, $p = 7.76 \times 10^{-3}$) and the 12th ring TWT ($\chi^2 = 4.57 \times 10^{-3}$, df = 1, $p = 0.98$). For ring width, the results showed that CBH mostly impacts intermediate rings, as its significance followed a concave curve starting with an increase from the 5th ring ($\chi^2 = 31.71$, df = 1, $p < 1e\text{-}5$) up until the 9th ring ($\chi^2 = 1045.15$, df = 1, $p < 1e\text{-}5$), then a decrease until the 13th ring ($\chi^2 = 40.19$, df = 1, $p < 10^{-5}$).

Trees that have a low CBH, i.e., fast growers, end up with a markedly larger DBH - though smaller at the beginning - and a slightly lower wood density, with no effect on TRW, TTW or TWT (Fig. 2C, S4): in the model (2), the effect of CBH on DBH sharply decreased from the 3rd ring ($1.75 \times 10^{-2} \pm 0.00684$) to the 13th ring ($-9.51 \times 10^{-2} \pm 0.0525$), slightly increased on wood density from the 3rd ring ($1.10 \times 10^{-2} \pm 0.00507$) to the 13th ring ($4.95 \times 10^{-2} \pm 0.0105$), and remained low for TRW, TTW, and TWT from the 3rd ring ($1.12 \times 10^{-2} \pm 0.00682$) to the 13th ring ($5.39 \times 10^{-3} \pm 0.0296$). Fast growers also had significantly larger 9th rings, as the effect of CBH on ring width followed a convex curve matching its concave significance, reaching its largest negative value at the 9th ring (-0.100 ± 0.0117). The effect of CBH was consistent among genetic clusters for every phenotype apart from DBH, where population structure was determinant. Excluding hybrids from CSE and ALP, populations from extreme latitudes (CSE and ALP) were more influenced by CBH than the other populations (RBA, NPL, and CEU). This trend was not correlated with the latitudinal gradient of DBH, where southern populations have a larger DBH with a higher standard deviation (Table S3).

Population structure is a good predictor of macroscopic phenotypes, but impedes the detection of underlying genetic variants

The phenotypes are structured by both family and genetic cluster, as intra-family (or intra-population) variance was significantly lower than when the family (or population) structure was shuffled (Supplementary materials, section B). Unlike the Principal Component Analysis (PCA) on raw phenotypes, after correcting for environmental factors with model (1), PCA on the estimated family effects showed a clear population structure (Fig. 3A): genetic clusters were disposed along the PC1 (57.5% of variance explained) in decreasing latitudinal order (from right to left), with the exception of CEU and ALP being reversed. PC1 was mostly driven by DBH, ring width and wood density, while PC2 (18.2% of variance explained) was mostly driven by TRW, TTW, and TTW.

At the 13th ring, population structure was mostly stronger for macroscopic than microscopic traits (Fig. 3B), as the significance of the genetic cluster effect in the model (2) was large for DBH and ring width ($\chi^2 > 131.26$, df = 5, $p < 10^{-5}$), intermediate for wood density and TWT ($\chi^2 > 79.51$, df = 5, $p < 10^{-5}$), and low for TRW and TTW ($\chi^2 < 19.39$, df = 5, $p < 10^{-2}$). Population structure was also stronger for later rings, as the analysis of variance showed an increasing significance over time for every phenotype ($t > 4.36$, $p < 0.00181$), apart from TRW ($t = -0.706$, $p < 0.498$) and TTW ($t = -2.63$, $p = 0.0274$).

In the GWASs on the 66 phenotypes (six phenotypes on 11 annual rings), population structure was as expected a confounding factor with genetic control, as peaks of significant SNPs were removed when correcting for population structure and/or kinship (Fig. 3C, 3D). When correcting for population structure and/or kinship in the GWASs (M*, K, or K*), estimated *p*-values followed a uniform distribution with a 95% confidence (Fig. 3E, 3F), as the distance D was negative for at least 64 out of 66 phenotypes. Only the 8th ring wood density had some SNPs more significant than expected (D = 0.0662), but none of the SNPs were significant after re-estimating the effect size with the adaptive shrinkage framework ($p > 0.201$). As a matter of fact, correcting our sample for population structure or kinship flattened, or even overcorrected the genetic signals on the Manhattan plots, since, when no

correction was applied, SNPs were more significant than expected for 41 out of 66 phenotypes. GWASs within the largest genetic cluster CSE were also inconclusive, as the distance D was also always negative (except for the 3rd ring wood density), with or without correcting for kinship (Fig. S5).

Discussion

A series of post-glacial demographic movements shaped the current population structure of Norway spruce in Europe (Tsuda et al., 2016; Chen et al., 2019). As the Swedish breeding program is a mixture of local trees and recent introductions from the natural range of Norway spruce, the progeny tests implemented across Sweden reflect the post-glacial population structure, and constitute a valuable resource for evolutionary biology. Through the analyses of DBH, wood density and tracheid traits on increment cores, the present paper shows that in terms of evolution and competition, the most important trait was as expected trait associated with growth - DBH - much more so than wood density or its components. We show that competitive abilities on DBH are population specific, and stronger in core populations close to their glacial refugia. Finally, we show that population structure for Norway spruce is intrinsically associated with latitude, and as such is a good predictor of adaptation but an impediment for detecting underlying genetic variants.

Competitive abilities was stronger in core populations

Phenotypes expressed in later stages of life are partly due to genetics, environment, and advantages acquired in early stages of life. Being a measure of the lag between the calendar age and the cambial age at BH, CBH is a proxy of the early growth rate, and studying its effect is an investigation of the consequence of acquiring early advantages. Every phenotype considered here is linked to fitness in one way or in another, but the low heritability and the high genetic and environmental variances of CBH suggests that it is more so than at least tracheid traits (Houle, 1992; p.235, Caballero, 2020).

A priori, there is no reason to believe that fast growers would be larger than slow growers for a given number of annual rings. In fact, in early stages of life, fast growers were slightly smaller. However, even if fast growers were smaller for a given cambial age, they were larger than slow growers for a given calendar age. Inevitably, from an intermediate number of annual rings - between the 5th and the 9th rings in our experiment - fast growers oversized slow growers: the taller stature reached earlier by fast growers gave them the upper hand in the competition for light and space resources, which came into play when planted trees reached a certain size. The cambial age at which the competition starts is most likely driven by the tree-to-tree distance, and increasing the distance will probably delay the competition. With a sufficiently large tree-to-tree distance, competition might never start, and a fast growth rate will never be advantageous. As a result, without competition, slow growers might be larger at later stages.

Early growth rate equally affected the different clusters, up until later stages of life where sensitivity to competition seemed to be longitudinally ordered: following the demographic model of Chen et al. (2019), and excluding CSE-ALP, the ability to benefit from early competition (high negative effect of CBH on DBH) in western populations (CSE, CEU and ALP) roughly increased westwards, whereas this ability in eastern populations (NPL and RBA) increased eastwards. In our experiment, populations seemed to have better

competitive abilities when they were close to their putative core populations. Such a trend can be due to successive bottlenecks during the expansion (Excoffier et al., 2008), and has been previously observed in many species (e.g., Riis et al., 2010; Van Wallendael et al., 2018; Orsucci et al., 2020). The ability to benefit from early competition to reach a larger size was not correlated to the size itself, as DBH was latitudinally ordered - southern populations being larger. The apparently evident latitudinal pattern might perhaps be divisible as well into western and eastern populations, but this hypothesis has to be further investigated with even more populations.

Population structure showed adaptation in resultant traits

In addition to the longitudinal component of the demographic model inferred by Chen et al. (2019), there is a latitudinal component at the genetic and phenotypic level, as previously reported (Milesi et al., 2019; Li et al., preprint). Since local adaptation often matches the environment (Savolainen et al., 2013) and colonization routes follow environmental gradients (Gaggiotti et al., 2009; Li et al, preprint), population structure of Norway spruce was as a result strongly confounded with local adaptation. Therefore, when assessing the genetic control underlying adaptation in Norway spruce, if not correcting for population structure, GWASs will increase the false positive rate (Barton et al., 2019; Lawson et al., 2020), and if correcting for population structure, GWASs will show no signal at all. Correctly assessing the genetic variants underlying the phenotypic variation is then not possible when there is such a strong latitudinal component. Increasing the number of samples or the number of SNPs remained inconclusive (Chen et al., 2021). Surprisingly, running a GWAS within one genetic cluster was also inconclusive, and suggests that all the adaptive signals are carried by the shift in allele frequencies between genetic clusters. A suggestion is to consider phenotypes that are less latitudinally associated, such as bud burst, and correct other phenotypes by the population structure thereby inferred (Milesi et al., 2019).

The other side of the coin is that population structure is a good predictor of adaptation. The strongest effect of population structure was observed for DBH and ring width, suggesting that most of the adaptation is linked with radial or upright growth. Moreover, DBH had a slightly higher Q_{ST} (0.201 at the 3rd ring to 0.358 to the 13th ring; see Supplementary materials, section D) than previously reported F_{ST} (0.116-0.145 from Table 1 of Chen et al. 2019), suggesting a divergence selection, and supporting the adaptation carried out by post-glacial clusters, but this hypothesis needs further studies. Wood density came second, and the significance of TWT was questionable as it was strongly correlated to wood density ($\rho = 0.88$). The PCA on family effects (Fig. 3A) also showed that the latitudinal component - and so, population structure - was mostly explained by DBH, ring width and wood density. The resulting pattern is that adaptation - or population structure - was more tightly linked to traits that are resultants rather than to its components, in agreement with Caballero (2020: p. 253). Indeed, components can have random variations as long as altogether, the resultant is fit for selection. Components have a higher degree of freedom, and therefore are more noisy. Since genetic polymorphism depicted by SNPs are partly linked to selection, genomic selection on resultant - such as DBH or wood density - should be much more efficient than on components - such as tracheid traits.

Acknowledgements

The authors acknowledge the Bio4Energy project and Skogforsk for access to phenotypic data, and the Swedish Foundation for Strategic Research (SSF), grant number RBP14-0040 for exome capture data. This study was funded by the following sources: Uppsala University, SLU Umeå, and the European Union's Horizon 2020 B4Est for basic functioning and postdoc grant for MT. The authors would also like to thank Sophie Karrenberg and Zhiqiang Chen for their useful feedback. The computations and data handling were enabled by resources provided by the Swedish National Infrastructure for Computing (SNIC) at UppMax partially funded by the Swedish Research Council through grant agreement no. 2018-05973.

References

Barton, N., Hermisson, J., and Nordborg, M. (2019). Why structure matters: Great care is needed when interpreting claims about the genetic basis of human variation based on data from genome-wide association studies. eLife, 8.

Bates, D., Mächler, M., Bolker, B. M., and Walker, S. C. (2014). Fitting linear mixed-effects models using lme4. Journal of Statistical Software, 67. Bergh, J., Linder, S., and Bergström, J. (2005). Potential production of norway spruce in sweden. Forest Ecology and Management, 204:1–10.

Bernhardsson, C., Vidalis, A., Wang, X., Scofield, D. G., Schiffthaler, B., Baison, J., Street, N. R., García-Gil, M. R., and Ingvarsson, P. K. (2019). An ultra-dense haploid genetic map for evaluating the highly fragmented genome assembly of norway spruce (picea abies). G3 Genes|Genomes|Genetics, 9:1623–1632.

Burton, O. J., Phillips, B. L., and Travis, J. M. (2010). Trade-offs and the evolution of life-histories during range expansion. Ecology Letters, 13:1210–1220.

Caballero, A.. 2020. Quantitative Genetics. Cambridge University Press. [p.235]

Case, T. J. (1990). Invasion resistance arises in strongly interacting species-rich model competition communities. Proceedings of the National Academy of Sciences, 87:9610–9614.

Case, T. J., Holt, R. D., McPeek, M. A., and Keitt, T. H. (2005). The community context of species' borders: ecological and evolutionary perspectives. Oikos, 108:28–46.

Chang, C. C., Chow, C. C., Tellier, L. C., Vattikuti, S., Purcell, S. M., and Lee, J. J. (2015). Second-generation plink: Rising to the challenge of larger and richer datasets. GigaScience, 4:7.

Chave, J., Coomes, D., Jansen, S., Lewis, S. L., Swenson, N. G., and Zanne, A. E. (2009). Towards a worldwide wood economics spectrum. Ecology Letters, 12:351–366.

Chen, J., Li, L., Milesi, P., Jansson, G., Berlin, M., Karlsson, B., Aleksic, J., Vendramin, G. G., and Lascoux, M. (2019). Genomic data provide new insights on the demographic history and the extent of recent material transfers in norway spruce. Evolutionary Applications, 12:1539–1551.

Chen, Z. Q., Zan, Y., Milesi, P., Zhou, L., Chen, J., Li, L., Cui, B. B., Niu, S., Westin, J., Karlsson, B., García-Gil, M. R., Lascoux, M., and Wu, H. X. (2021). Leveraging breeding programs and genomic data in norway spruce (picea abies l. karst) for gwas analysis. Genome Biology, 22:1–30.

de Villemereuil, P., Gaggiotti, O. E., and Goudet, J. (2020). Common garfen experiments to study local adaptation need to account for population structure. Journal of Ecology.

der Auwera, G. A. V., Carneiro, M. O., Hartl, C., Poplin, R., del Angel, G., Levy-Moonshine, A., Jordan, T., Shakir, K., Roazen, D., Thibault, J., Banks, E., Garimella, K. V., Altshuler, D., Gabriel, S., and DePristo, M. A. (2013). From fastq data to high-confidence variant calls: The genome analysis toolkit best practices pipeline. Current Protocols in Bioinformatics, 43:11.10.1–11.10.33.

Enquist, B. J., West, G. B., Charnov, E. L., and Brown, J. H. (1999). Allometric scaling of production and life-history variation in vascular plants. Nature 1999 401:6756, 401:907–911.

Falster, D. S. (2006). Sapling strength and safety: the importance of wood density in tropical forests. New Phytologist, 171:237–239.

Falster, D. S. and Westoby, M. (2003). Plant height and evolutionary games. Trends in Ecology & Evolution, 18:337–343.

Falster, D. S. and Westoby, M. (2005). Alternative height strategies among 45 dicot rain forest species from tropical queensland, australia. Journal of Ecology, 93:521–535.

Gelder, H. A. V., Poorter, L., and Sterck, F. J. (2006). Wood mechanics, allometry, and life-history variation in a tropical rain forest tree community. New Phytologist, 171:367–378.

Givnish, T. J. (2015). On the adaptive significance of leaf height in forest herbs. https://doi.org/10.1086/283995, 120:353–381.

Hewitt, G. (2000). The genetic legacy of the quaternary ice ages. Nature 2000 405:6789, 405:907–913.

Hewitt, G. M. (1996). Some genetic consequences of ice ages, and their role in divergence and speciation. Biological Journal of the Linnean Society, 58:247–276.

Iwasa, Y., Cohen, D., and Leon, J. A. (1985). Tree height and crown shape, as results of competitive games. Journal of Theoretical Biology, 112:279–297. K, K. (1994). Relative importance of photosynthetic traits and allocation patterns as correlates of seedling shade tolerance of 13 tropical trees. Springer.

Kawecki, T. J. and Ebert, D. (2004). Conceptual issues in local adaptation. Ecology Letters, 7:1225–1241.

Lawson, D. J., Davies, N. M., Haworth, S., Ashraf, B., Howe, L., Crawford, A., Hemani, G., Smith, G. D., and Timpson, N. J. (2019). Is population structure in the genetic biobank era irrelevant, a challenge, or an opportunity? Human Genetics 2019 139:1, 139:23–41.

Li, H., Handsaker, B., Wysoker, A., Fennell, T., Ruan, J., Homer, N., Marth, G., Abecasis, G., and Durbin, R. (2009). The sequence alignment/map format and samtools. Bioinformatics, 25:2078–2079.

Lundqvist, S. O., Seifert, S., Grahn, T., Olsson, L., García-Gil, M. R., Karlsson, B., and Seifert, T. (2018). Age and weather effects on between and within ring variations of number, width and coarseness of tracheids and radial growth of young norway spruce. European Journal of Forest Research, 137:719–743.

McKenna, A., Hanna, M., Banks, E., Sivachenko, A., Cibulskis, K., Kernytsky, A., Garimella, K., Altshuler, D., Gabriel, S., Daly, M., and DePristo, M. A. (2010). The genome analysis toolkit: A mapreduce framework for analyzing next-generation dna sequencing data. Genome Research, 20:1297–1303.

Milesi, P., Berlin, M., Chen, J., Orsucci, M., Li, L., Jansson, G., Karlsson, B., and Lascoux, M. (2019). Assessing the potential for assisted gene flow using past introduction of norway spruce in southern sweden: Local adaptation and genetic basis of quantitative traits in trees. Evolutionary Applications, 12:1946–1959.

Niklas, K. J. (1993). Influence of tissue density-specific mechanical properties on the scaling of plant height. Annals of Botany, 72:173–179.

Nystedt, B., et al. (2013). The norway spruce genome sequence and conifer genome evolution. Nature 2013 497:7451, 497:579–584.

Palmé, A. E., Su, Q., Rautenberg, A., Manni, F., and Lascoux, M. (2003b). Postglacial recolonization and cpdna variation of silver birch, betula pendula. Molecular Ecology, 12:201–212.

Petit, R., Aguinagalde, I., de Beaulieu, J., . . . , C. B., and undefined 2003 (1003). Glacial refugia: hotspots but not melting pots of genetic diversity. science.sciencemag.org.

Poorter, L., Bongers, L., and Bongers, F. (2006). Architecture of 54 moist-forest tree species: traits, trade-offs, and functional groups. Ecology, 87:1289–1301.

Poorter, L., McDonald, I., Alarcón, A., Fichtler, E., Licona, J. C., Peña-Claros, M., Sterck, F., Villegas, Z., and Sass-Klaassen, U. (2010). The importance of wood traits and hydraulic conductance for the performance and life history strategies of 42 rainforest tree species. New Phytologist, 185:481–492.

Pretzsch, H., Biber, P., Schütze, G., Kemmerer, J., and Uhl, E. (2018). Wood density reduced while wood volume growth accelerated in central european forests since 1870. Forest Ecology and Management, 429:589–616.

Provan, J. and Bennett, K. D. (2008). Phylogeographic insights into cryptic glacial refugia. Trends in Ecology & Evolution, 23:564–571.

R Core Team (2021). R: A language and environment for statistical computing. R Foundation for Statistical Computing, Vienna, Austria. URL: https://www.R-project.org/.

Rossi, S., Cairo, E., Krause, C., and Deslauriers, A. (2015). Growth and basic wood properties of black spruce along an alti-latitudinal gradient in quebec, canada. Annals of Forest Science, 72:77–87.

Saccheri, I. and Hanski, I. (2006). Natural selection and population dynamics. Trends in Ecology & Evolution, 21:341–347.

Savolainen, O., Lascoux, M., and Merilä, J. (2013). Ecological genomics of local adaptation. Nature Reviews Genetics 2013 14:11, 14:807–820.

Evans, R., and Ilic, J. (2001). Application of near infrared spectroscopy to a diverse range of species demonstrating wide density and stiffness variation. IAWA Journal, 22:415–429.

Sedmáková, D., Sedmák, R., Bosela, M., Ježík, M., Blaženec, M., Hlásny, T., and Marušák, R. (2019). Growth-climate responses indicate shifts in the competitive ability of european beech and norway spruce under recent climate warming in east-central europe. Dendrochronologia, 54:37–48.

Stephens, M. (2017). False discovery rates: a new deal. Biostatistics, 18:275–294.

M. Tiret, P. Milesi, Statistical Peak Detection for GWAS. Zenodo. https://doi.org/10.5281/zenodo.5079556. Deposited 7 July 2021.

Vendramin, G. G., Anzidei, M., Madaghiele, A., Sperisen, C., and Bucci, G. (2000). Chloroplast microsatellite analysis reveals the presence of population subdivision in norway spruce (picea abies k.). https://doi.org/10.1139/g99-093, 43:68–78.

Vidalis, A., Scofield, D. G., Neves, L. G., Bernhardsson, C., García-Gil, M. R., & Ingvarsson, P. K. (2018). Design and evaluation of a large sequence-capture probe set and associated SNPs for diploid and haploid samples of Norway spruce (Picea abies). *BioRxiv*, 291716.

Yang, J., Lee, S. H., Goddard, M. E., and Visscher, P. M. (2011). Gcta: A tool for genome-wide complex trait analysis. The American Journal of Human Genetics, 88:76–82.

Figure legends and Tables

Figure 1. Overall phenotypes and genotypes of the sample of *Picea abies*. (A) Principal Component Analysis of the phenotypes: Diameter at Breast Height (DBH), Ring Width (RW), Wood Density (WD), Tracheid Radial Width (TRW), Tracheid Tangential Width (TTW), and Tracheid Wall Thickness (TWT). Left panel only shows variable axes and 60% confidence ellipses. Each data (dot) on the right panel is colored according to its cambial age (3rd year in light blue up until 13th year in dark blue). PC1 and PC2 explained 41.2% and 38.3% of the variance respectively. **(B)** Principal Component Analysis of the genotypes of the half-sib families. Families are colored according to their genetic clusters (ordered by decreasing latitude in the legend): Central and South Sweden (CSE, dark red), Russia-Baltics (RBA, light green), Northern Poland (NPL, green), Central Europe (CEU, light blue), Alpines (ALP, blue), and hybrids between CSE and ALP (CSE-ALP, pink). PC1 and PC2 explained 3.42% and 0.45% of the variance respectively. **(C)** Admixture plot of the half-sib families, with K = 3. Individuals are grouped by population, and sorted according to their coancestry coefficient.

Figure 2. Effect of Calendar age at Breast Height (CBH) on *Picea abies*. (A) Boxplots of predicted CBH according to model (1bis) as a function of site (Horeda in light blue, Erikstorp in dark blue) and of genetic cluster: Central and South Sweden (CSE), Russia-Baltics (RBA), Northern Poland (NPL), Central Europe (CEU), Alpines (ALP), and hybrids between CSE and ALP (CSE-ALP). **(B)** ANOVA of CBH in model (2) as a function of cambial age (from 3 to 13), and of trait: Diameter at Breast Height (DBH, plain circle), Ring Width (RW, plain triangle), Wood Density (WD, plain square), Tracheid Radial Width (TRW, circle), Tracheid Tangential Width (TTW, triangle), and Tracheid Wall Thickness (TWT, square). **(C)** Estimated effect of CBH in model (2) as a function of cambial age (from 3 to 13), and of trait (idem as panel B), in the trial of Höreda.

Figure 3. Genetic control of wood properties in *Picea abies*. (A) Principal Component Analysis of the residuals of the phenotypes according to model (2): Diameter at Breast Height (DBH), Ring Width (RW), Wood Density (WD), Tracheid Radial Width (TRW), Tracheid Tangential Width (TTW), and Tracheid Wall Thickness (TWT). Left panel only shows variable axes and 10% confidence ellipses (zoomed x2.5). Each data (dot) on the right panel is colored according to its genetic cluster (ordered by decreasing latitude in the legend): Central and South Sweden (CSE, dark red), Russia-Baltics (RBA, light green), Northern Poland (NPL, green), Central Europe (CEU, light blue), Alpines (ALP, blue), and hybrids between CSE and ALP (CSE-ALP, pink). PC1 and PC2 explained 57.5% and 18.2% of the variance respectively. **(B)** ANOVA of genetic clusters in model (2) as a function of cambial age (from 3 to 13), and of trait: DBH (plain circle), RW (plain triangle), WD (plain square), TRW (circle), TTW (triangle), and TWT (square). **(C)** Manhattan plot of the GWAS in model (M) of DBH at the 5th ring. The dotted horizontal line is the Bonferroni significance level for n = 118,145. The dashed vertical lines are the location of the peaks of significant SNPs. **(D)** Manhattan plot of the GWAS in model (M*) of DBH at the 5th ring. Legends are identical to panel C. **(E)** Q-Q plot of observed *versus* expected *p*-values (in log scale) on the 5th ring DBH, without any correction (M, in squares), with population structure correction (M*, in plain squares), with kinship correction (K, in circles), and with population structure and kinship corrections (K*, in plain circles). The solid line is 1-slope line, and the dashed lines are the upper and lower bound of the 95% confidence interval. **(F)** Distance *D* on

GWAS (K*) as a function of cambial age and of traits (idem than panel B). The dotted horizontal lines indicate the width of the 95% confidence interval.

	CBH (year)	**DBH (mm)**	**ring width (mm)**	**wood density ($kg.m^{-3}$)**	**TRW (µm)**	**TTW (µm)**	**TWT (µm)**
CSE	5.12 ± 1.44	91.82 ± 21.86	2.16 ± 1.03	456.49 ± 65.92	29.14 ± 2.27	28.29 ± 1.85	2.30 ± 0.31
RBA	5.03 ± 1.37	91.37 ± 21.01	2.18 ± 1.04	445.32 ± 60.51	29.29 ± 2.46	28.12 ± 1.75	2.24 ± 0.29
NPL	4.90 ± 1.22	100.98 ± 23.56	2.60 ± 1.18	437.40 ± 57.42	29.89 ± 2.16	28.76 ± 1.73	2.25 ± 0.28
CEU	4.83 ± 1.37	105.95 ± 23.62	2.70 ± 1.12	419.43 ± 59.36	29.84 ± 2.36	28.90 ± 1.84	2.14 ± 0.28
CSE-ALP	4.89 ± 1.24	97.06 ± 21.23	2.47 ± 1.14	435.63 ± 64.59	29.60 ± 2.40	28.43 ± 1.78	2.21 ± 0.29
ALP	4.86 ± 1.34	103.18 ± 24.36	2.67 ± 1.20	432.55 ± 59.37	29.62 ± 2.33	28.50 ± 1.94	2.20 ± 0.28
σ_F^2	1.90×10^{-3}	3.03×10^{-2}	5.13×10^{-3}	2.77×10^{-3}	5.99×10^{-4}	4.73×10^{-4}	2.47×10^{-3}
$\sigma_B^2 + \sigma^2$	3.29×10^{-2}	2.15×10^{-1}	5.63×10^{-2}	1.95×10^{-2}	6.04×10^{-3}	4.91×10^{-3}	1.88×10^{-2}
h^2 (%)	5.22	12.33	8.37	12.45	9.03	8.80	11.63

Table 1. The average value and the standard deviation of each phenotype at the 13th annual rings, for each genetic cluster: Central and South Sweden (CSE), Russia-Baltics (RBA), Northern Poland (NPL), Central Europe (CEU), Alpines (ALP), and hybrids between CSE and ALP (CSE-ALP). Genetic variance (σ_F^2), environmental variance ($\sigma_B^2 + \sigma^2$), and heritability (h^2) were estimated with model (1).

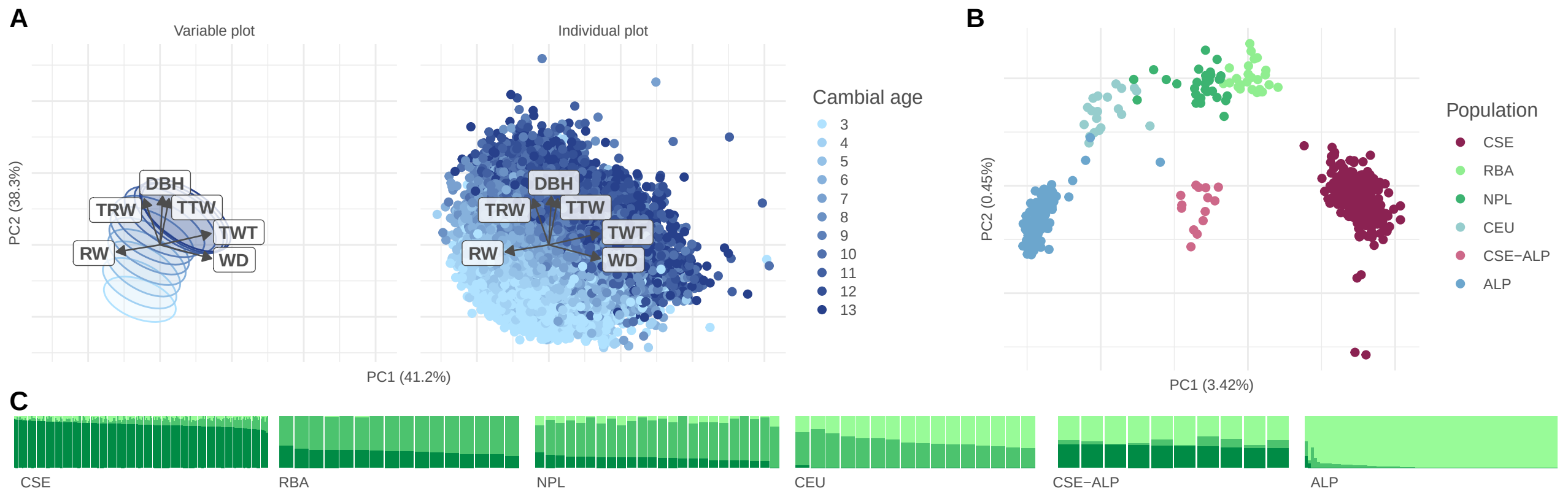
A
Variable plot
Individual plot
DBH
TRW
TTW
TWT
RW
WD
PC2 (38.3%)
PC1 (41.2%)
Cambial age
3
4
5
6
7
8
9
10
11
12
13
B
PC2 (0.45%)
PC1 (3.42%)
Population
CSE
RBA
NPL
CEU
CSE−ALP
ALP
C
CSE
RBA
NPL
CEU
CSE−ALP
ALP

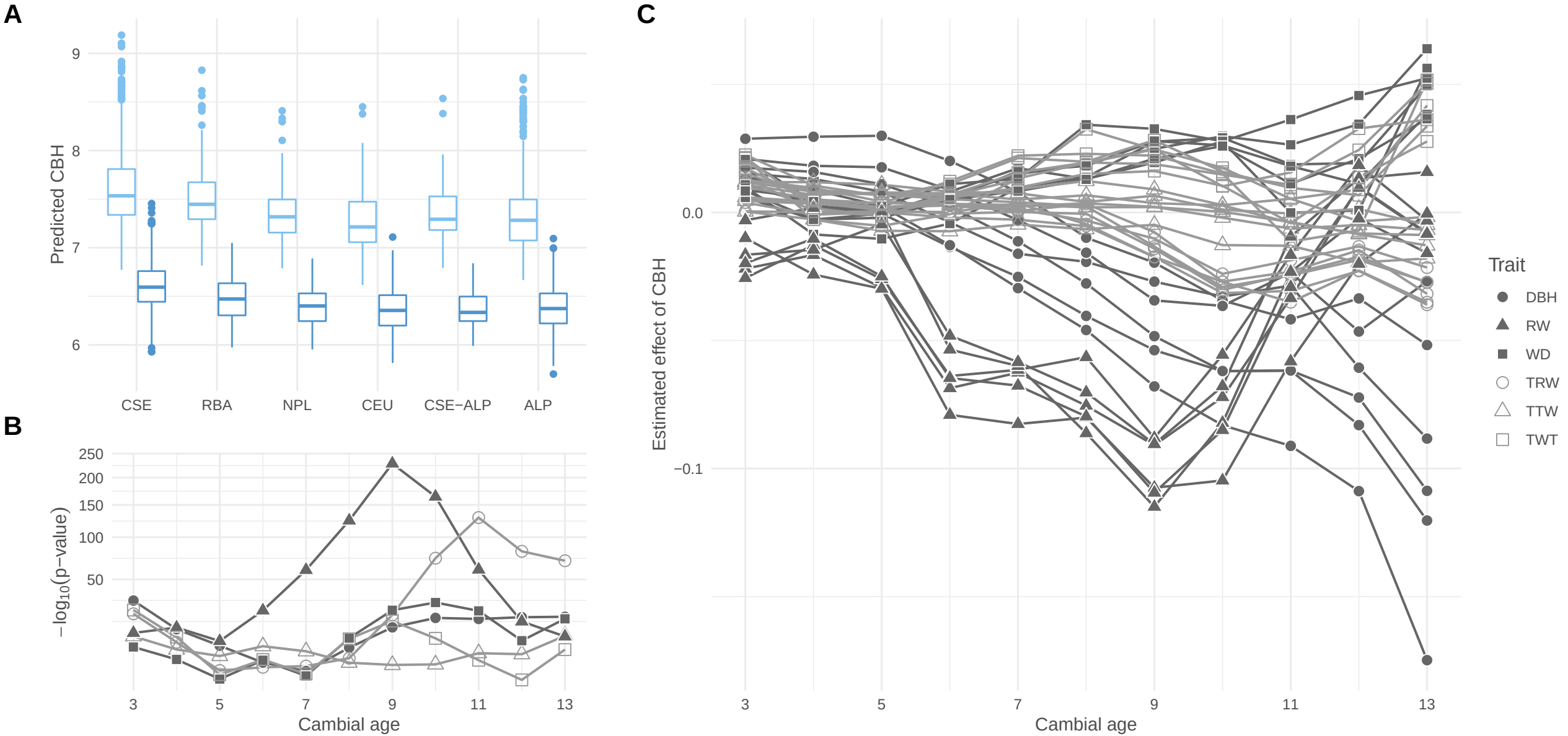
A
Predicted CBH
9
8
7
6
CSE
RBA
NPL
CEU
CSE−ALP
ALP
B
−log10(p−value)
250
200
150
100
50
3
5
7
9
11
13
Cambial age
C
Estimated effect of CBH
0.0
−0.1
3
5
7
9
11
13
Cambial age
Trait
DBH
RW
WD
TRW
TTW
TWT

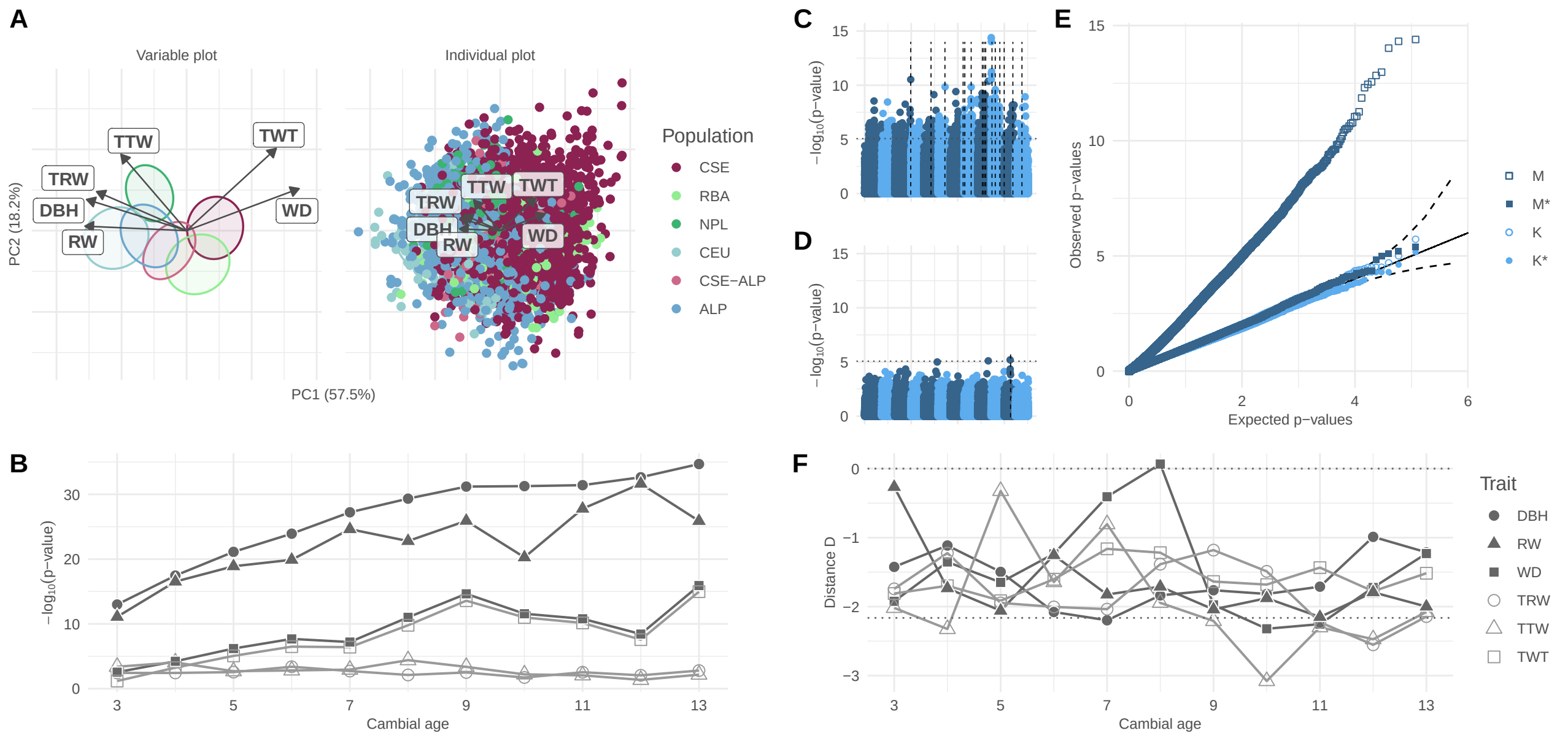
A
Variable plot
Individual plot
TTW
TWT
TRW
DBH
RW
WD
PC2 (18.2%)
PC1 (57.5%)
Population
CSE
RBA
NPL
CEU
CSE−ALP
ALP
C
D
−log10(p−value)
E
Observed p−values
Expected p−values
M
M*
K
K*
B
Cambial age
F
Distance D
Trait
DBH
RW
WD
TRW
TTW
TWT